JSHC
Japan Society of
Histochemistry and Cytochemistry
Established 1959

Acta Histochem. Cytochem. 48 (4): 125–133, 2015
doi: 10.1267/ahc.14066

Localization of Nitric Oxide Synthase-containing Neurons in the Bat Visual Cortex and Co-localization with Calcium-binding Proteins

Ya-Nan Gu[1], Hang-Gu Kim[1] and Chang-Jin Jeon[1]

[1]Department of Biology, School of Life Sciences, BK21 Plus KNU Creative BioResearch Group, College of Natural Sciences, and Brain Science and Engineering Institute, Kyungpook National University, Daegu, 41566, South Korea

Received December 23, 2014; accepted July 15, 2015; published online August 20, 2015

Microchiroptera (microbats) is a suborder of bats thought to have degenerated vision. However, many recent studies have shown that they have visual ability. In this study, we labeled neuronal nitric oxide synthase (nNOS)—the synthesizing enzyme of the gaseous non-synaptic neurotransmitter nitric oxide—and co-localized it with calbindin D28K (CB), calretinin (CR), and parvalbumin (PV) in the visual cortex of the greater horseshoe bat (*Rhinolophus ferrumequinum*, a species of microbats). nNOS-immunoreactive (IR) neurons were found in all layers of the visual cortex. Intensely labeled neurons were most common in layer IV, and weakly labeled neurons were most common in layer VI. Majority of the nNOS-IR neurons were round- or oval-type neurons; no pyramidal-type neurons were found. None of these neurons co-localized with CB, CR, or PV. However, the synthesis of nitric oxide in the bat visual cortex by nNOS does not depend on CB, CR, or PV.

Key words: nitric oxide synthase, immunocytochemistry, localization, visual cortex, calcium-binding protein

I. Introduction

"Bat" is the general term used to describe the order *Chiroptera*, which comprises a species of mammals with sustained flying ability. It is the second largest mammalian order after rodents. To date, about 1,000 species have been found globally, except in the polar regions. The order includes two major suborders: *Megachiroptera* (megabats) and *Microchiroptera* (microbats). The megabats (~150 species identified) are larger with large eyes and excellent vision; most of them are frugivorous. The microbats (~850 species identified) are smaller with small eyes and are thought to identify objects by echolocation. Most of them are insectivorous. The greater horseshoe bat (*Rhinolophus ferrumequinum*) is one such species. They are insectivorous, cave dwelling and nocturnal like other species of microbats. Although considered blind like other microbats, they still have eyes that receive external visual information and play an important role in visual pathways. Therefore, whether microbats are blind or retain their vision has recently attracted investigators. Numerous studies, considering various aspects have shown that microbats have vision [21, 22, 24, 31, 42, 44]. However, the characteristics of their visual cortices are poorly understood.

Findings in the past few decades have shown that nitric oxide (NO) is a gaseous retrograde messenger in the nervous system of mammals. It has also been recognized as a toxic gas and major atmospheric pollutant [5, 15]. NO transmits signals between both, heterosynapses (synapses between homoneurons) and heteroneurons [6, 14, 30]. In addition, it is an important non-synaptic neurotransmitter [11, 12, 25, 38, 39, 40]. It is an extremely diffusible non-polar gas that can cross biological membranes easily and transfer signals over a few hundred micrometers in a short time [15]. NO is synthesized by neuronal nitric oxide synthase (nNOS) from L-arginine with the cofactor nicotinamide adenine dinucleotide phosphate (NADPH) and O_2 in the nervous system of mammals [7, 11]. nNOS is one of three types of NOS involved in the regulation of nervous

Correspondence to: Prof. Chang-Jin Jeon, Neuroscience Lab., Department of Biology, College of Natural Sciences, Kyungpook National University, 80, Daehak-ro, Daegu, 41566, South Korea.
E-mail: cjjeon@knu.ac.kr

system function. The other two types are the cardiovascular function-related endothelial NOS (eNOS) and immune function-related inducible NOS (iNOS) [17, 37]. nNOS is a calmodulin-dependent enzyme [8, 11]. Both the synthesis and release of NO in the nervous system rely on an increase in intracellular calcium [11, 15, 17, 25].

Calcium ions play an important modulatory role in many biological processes. Calcium-binding proteins (CBPs) regulate or mediate the intracellular activity of calcium ions [3, 36]. Therefore, impairments in calcium regulation by CBPs influence many intracellular calcium dynamics (balance) and cause neurodegenerative diseases [2, 4, 9, 13, 18, 19, 20, 28, 34]. Although the physiological functions of CBPs are not yet clear, they are frequently used as neuronal subpopulation markers because of their specificity to different subpopulations of neurons. In addition, they have been suggested to be involved in different calcium-dependent processes [10, 35, 41].

Microbats are known to have AII amacrine cells [21], M/L [24] and S cone photoreceptors [31] in their retina, suggesting that they have retained the anatomical structure associated with bright- and dim-light vision and dichromatic color identification [21, 24, 31]. In addition, we recently localized calbindin D28K (CB)-, calretinin (CR)-, and parvalbumin (PV)-immunoreactive (IR) neurons in the bat superior colliculus [22]. These studies provide new evidence for the possibility of vision. In addition, numerous studies have proven the visual ability of bats with behavioristics [42] and genetics [44].

To the best of our knowledge, there are no studies of the bat visual cortex in the fields of neurology and histology. Therefore, the present study aimed to examine if nNOS-IR neurons were localized in specific lamina and cell types and to contrast the findings with those of previous studies in order to understand species diversity.

II. Materials and Methods

Animal and tissue preparation

Adult greater horseshoe bats (*R. ferrumequinum*) were used in this study. The bats were anesthetized deeply with a mixture of ketamine hydrochloride (30–40 mg/kg) and xylazine (3–6 mg/kg) before perfusion. All bats were perfused intracardially with 4% paraformaldehyde and 0.3–0.5% glutaraldehyde in 0.1 M sodium phosphate buffer (pH 7.4) containing 0.002% calcium chloride. Following a prerinse with approximately 10 ml of phosphate-buffered saline (PBS, pH 7.4) over a period of 3 min, each bat was perfused with 30 ml of fixative for 20–30 min via a syringe needle inserted through the left ventricle and aorta. The animal was decapitated and the head was placed in a fixative for 2–3 hr. The brain was then removed from the skull, stored for 2–3 hr in the same fixative and left overnight in 0.1 M phosphate buffer (pH 7.4) containing 8% sucrose and 0.002% $CaCl_2$. The brain was dissected and the visual cortex was isolated. It was mounted onto a chuck and cut into 50-μm thick sections with a Vibratome 3000 Plus sectioning system (Vibratome, St. Louis, MO, USA). The guideline of the National Institutes of Health for the Care and Use of Laboratory Animals were followed for all experimental procedures. All efforts were made to minimize animal suffering as well as the number of animals used.

Horseradish peroxidase immunocytochemistry

Polyclonal and monoclonal antibodies against nNOS were obtained from BD Biosciences (San Jose, CA, USA). The tissue was processed free floating in small vials. For immunocytochemistry, the sections were incubated in 1% sodium borohydride ($NaBH_4$) for 30 min. Sections were rinsed 3×10 min in PBS, incubated in PBS with 4% normal serum (normal goat serum for polyclonal antibody against nNOS and normal horse serum for monoclonal antibody against nNOS) for 2–10 hr with 0.5% Triton X-100 added. Sections were then incubated in the primary antiserum in PBS with 4% normal serum for 1–3 days with 0.5% Triton X-100 added. The primary antiserum was diluted 1:1000. Following 3×10 min rinses in PBS, sections were incubated in a 1:200 dilution of biotinylated secondary IgG in PBS with 4% normal serum for 2–10 hr with 0.5% Triton X-100 added. Sections were then rinsed 3×10 min in PBS and incubated in a 1:50 dilution of avidin-biotinylated horseradish peroxidase (Vector Labs., Burlingame, CA, USA) in PBS for 2–10 hr. The sections were again rinsed in 0.25 M Tris for 3×10 min. Finally, the staining was visualized by reacting with 3,3'-diaminobenzidine tetrahydrochloride (DAB) and hydrogen peroxide in 0.25 M Tris for 2–12 min using a DAB reagent set (Kirkegaard & Perry, Gaithersburg, MD, USA). All sections were then rinsed in 0.25 M Tris before mounting. Following the immunocytochemical procedures, the tissue was mounted on Superfrost Plus slides (Fisher, Pittsburgh, PA, USA) and dried overnight in a 37°C oven. The mounted sections were dehydrated through alcohol, cleared with xylene, and coverslipped with the mounting medium, Permount (Fisher). The sections were examined and photographed on a Zeiss Axioplan microscope (Carl Zeiss Meditec Inc., Jena, Germany) with conventional or differential interference contrast (DIC) optics.

Fluorescence immunocytochemistry

A polyclonal antibody against nNOS was obtained from BD Biosciences. Monoclonal antibodies against CB, CR or PV were obtained from Sigma (St. Louis, MO, USA). The tissue was processed free floating in small vials. For double-label sections with nNOS and CB, CR or PV, sections were incubated in 1% $NaBH_4$ for 30 min. Sections were rinsed 3×10 min in PBS, incubated in PBS with 4% normal serum (normal goat serum for both nNOS, CB, CR and PV) for 2 hr with 0.5% Triton X-100 added. Sections were then incubated in the primary antiserum in PBS with 4% normal serum for 48 hr with 0.5% Triton X-100 added.

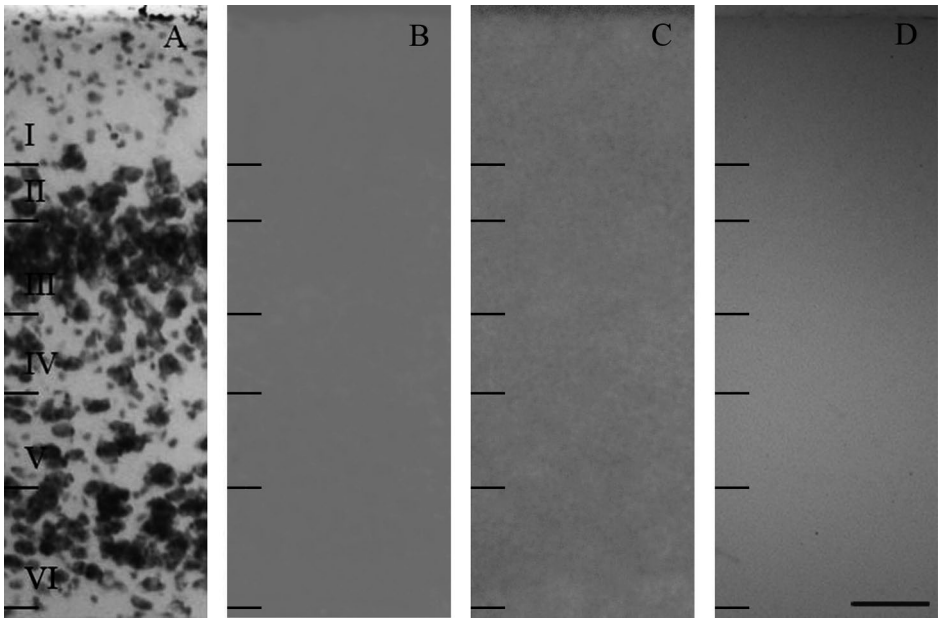

Fig. 1. Low-power photomicrographs of the preabsorption and negative controls of nNOS-IR neurons in the bat visual cortex. (**A**) Thionin-stained section showing cortical lamination. (**B**) Preabsorption control of rabbit antibody against nNOS. (**C**) Preabsorption control of mouse antibody against nNOS. (**D**) Negative control. The control tissues showed no nNOS immunoreactivity. Bar=100 μm.

The primary antibodies were diluted 1:500–1:1000 (nNOS) or 1:500 (CB, CR, PV). For detection by immunofluorescence, the secondary antibodies were fluorescein isothicyanate (FITC)-conjugated anti-rabbit IgG (Vector Labs.) for the anti-nNOS antibody and Cy3-conjugated anti-mouse (Jackson ImmunoResearch Laboratories, Inc., Baltimore, PA, USA) for anti-CB, CR, or PV antibodies. Following 3×10 min rinses in PBS, sections were incubated in the secondary antibodies in PBS with 4% normal serum (normal goat serum for both nNOS, CB, CR and PV) for 10 hr with 0.5% Triton X-100 added. Sections were then rinsed 3×10 min in PBS and the labeled sections were coverslipped with Vectashield mounting medium (Vector Labs.). Images were obtained with a Zeiss LSM700 laser scanning confocal microscope (Carl Zeiss Meditec Inc.)

Specificity of antibodies

To demonstrate the specificity of the immunoreaction, we performed two experiments: preabsorption control tests and a negative control test in the visual cortex of bat.

(1) Preabsorption control test

Preabsorption of anti-nNOS with the corresponding synthetic peptides (ChinaPeptides, Shanghai, China, human aa.1095–1289) were performed prior to tissue incubation. Blocking peptide of anti-nNOS was mixed with primary antibody at 10:1 ratio for 12 hr at room temperature to inactive the primary antibody and tissues were incubated with the preabsorbed antibody in place of the primary antibody. These control tissue showed no nNOS immunoreactivity (Fig. 1B and 1C).

(2) Negative control test

Some bat visual cortex sections were incubated in the same solution without the addition of the primary antibody. These control tissues showed no nNOS immunoreactivity (Fig. 1D).

Quantitative analysis

The average diameter, area of labeled cells, and cell counts were computed with a Zeiss AxioCam HRc digital camera (Axio Vision 4; Carl Zeiss Meditec Inc.). For each of the three animals, we analyzed 18 best-labeled sections that were 1500 μm in width across the superior-inferior extent of the visual cortex. The fields were positioned in the central visual cortex. A cursor was moved manually around the outer contour of each cell with a digital camera. The analysis was performed with a 63× Zeiss Plan-Apochromat objective. To show the laminar distribution of nNOS-IR neurons in bat visual cortex a little more visually the low-power photomicrographs showed in Figure 2. Were photograph with 20× Zeiss Plan-Apochromat objectives. To obtain the best images, we analyzed the cells with DIC optics. Only cells containing a nucleus with a nucleolus that was at least faintly visible were included in the analysis.

To determine the number of double-labeled cells, we counted fields 1500 μm in width across the superior-inferior extent of the visual cortex from 27 different sections selected from three different animals. The fields were positioned in the central visual cortex. Double-labeled images were obtained and viewed with a Zeiss LSM700 laser scanning confocal microscope (Carl Zeiss Meditec Inc.) with a 20× objective.

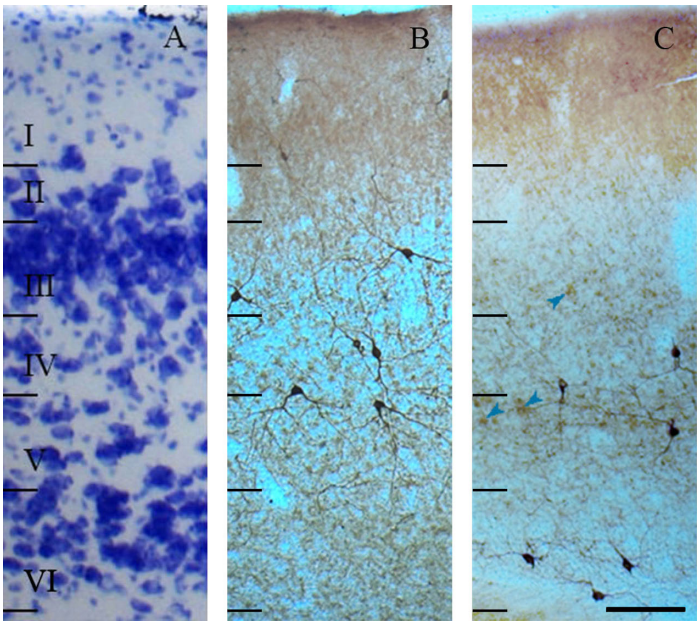

Fig. 2. Low-power photomicrographs of the laminar distribution of nNOS-IR neurons in the bat visual cortex. (**A**) Thionin-stained section showing cortical lamination. (**B** and **C**) nNOS-IR neurons. nNOS-IR neurons were only found in a small subset in the bat visual cortex that exhibited two different types of labeling. Notice the two different labeling densities of the nNOS-IR neurons. Arrowheads indicate weakly labeled neurons. The Roman numerals on the left side of this figure indicate the layers of visual cortex. Bar=100 μm.

III. Results

The distribution of nNOS-IR neurons in the bat visual cortex

Figure 2A shows a thionin-stained section that depicts cortical lamination, while Figures 2B and 2C show the nNOS-IR neurons. Two types of nNOS-IR neurons were observed in the bat visual cortex. The first type of neurons were intensely labeled, and the second type were weakly labeled (Fig. 2C, arrowhead). The large majority of nNOS-IR neurons were intensely labeled in the bat visual cortex (five times the immunoreactivity of the weakly labeled neurons). These were located mainly in layer IV, and the highest density of weakly labeled nNOS-IR neurons was in layer VI. Quantitative maps of the cell distribution revealed the density of the nNOS-IR neurons in each layer (Fig. 3). As a percentage of the total population of labeled neurons, 11.76% of the intensely labeled nNOS-IR neurons were found in layer I, 7.35% were in layer II, 18.63% in layer III, 25.00% in layer IV, 20.10% in layer V, and 17.16% in layer VI. While 10.64% of the weakly labeled nNOS-IR neurons were found in layer I, 19.15% in layer II, 17.02% in layer III, 14.89% in layer IV, 17.02% in layer V, and 21.28% in layer VI.

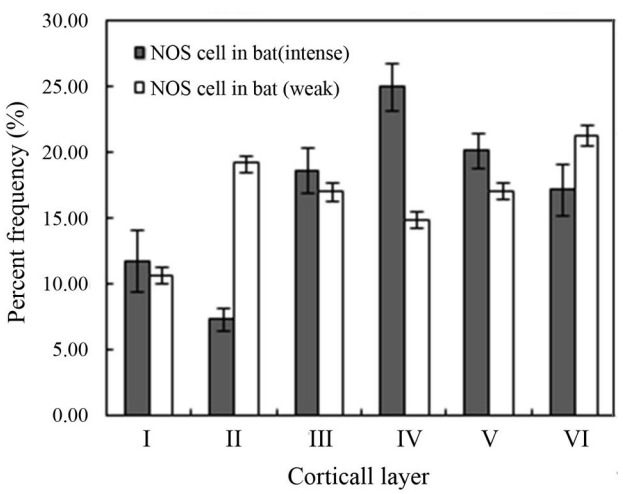

Fig. 3. Histogram of the percent frequency of laminar distribution of nNOS-IR neurons in the bat visual cortex. The intensely labeled nNOS-IR neurons were located mainly in layer IV, and the weakly labeled nNOS-IR neurons were located mainly in layer VI.

Morphology of the nNOS-IR neurons in the bat visual cortex

In the present study, we focused on the morphology of the intensely labeled nNOS-IR neurons because the soma and processes of the weakly labeled neurons were difficult to distinguish. Four types of nNOS-IR neurons were found in the bat visual cortex. Figure 4 shows representative neurons of each type.

The large majority of nNOS-IR neurons were round- or oval-type neurons with round or oval somas and many dendrites coursing all directions. Figures 4A, 4B, and 4C show representative multipolar round- or oval-type neurons. The other major type was stellate-type neurons with polygonal-shaped somas and many dendrites coursing all directions (Fig. 4D and 4E). Figures 4G and 4H show a representative vertical fusiform-type neuron having a vertical fusiform soma and a main long process ascending towards the pial surface and a long descending process.

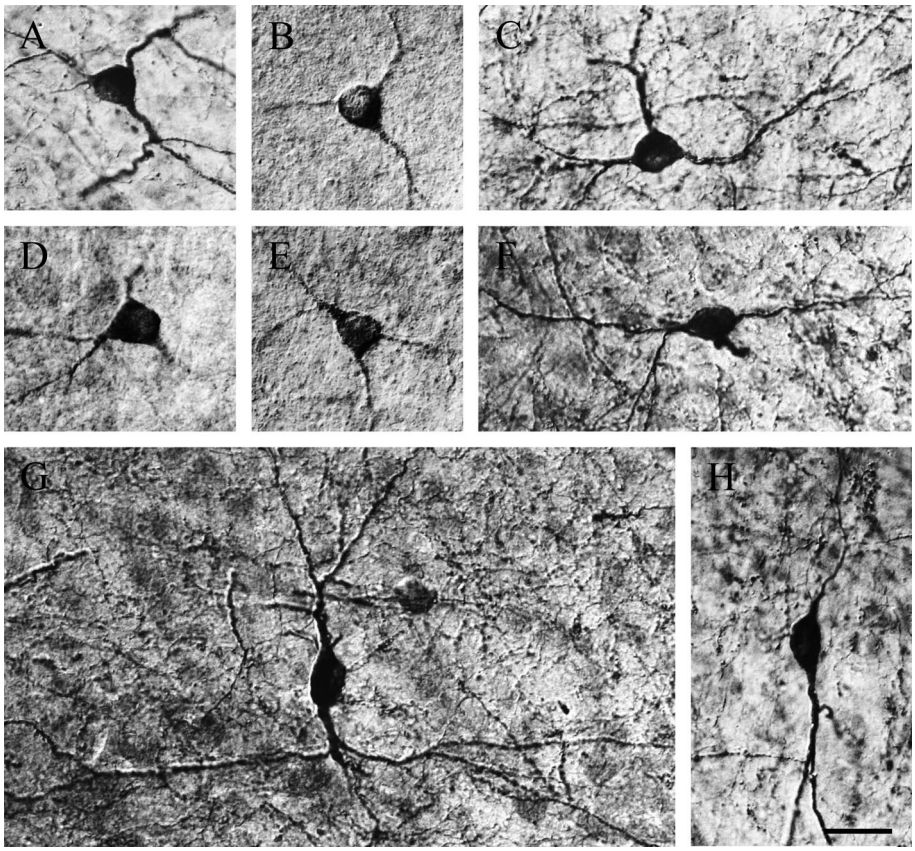

Fig. 4. High-power differential interference contrast (DIC) photomicrographs of some nNOS-IR neurons in the bat visual cortex. (**A, B, C**) Multipolar round- or oval-type neurons. Majority of nNOS-IR neurons in the bat visual cortex had round- or oval-shaped soma and multipolar dendrites. (**D, E**) Multipolar stellate-type neurons with polygonal-shaped somas and multipolar dendrites. (**F**) Horizontal-type neuron with horizontal round- to spindle-shaped soma and horizontal processes from two opposite poles of the soma. (**G, H**) Vertical fusiform-type neurons with vertical fusiform-shaped soma and vertical processes from two opposite poles of the soma and perpendicular to the pial surface. Bar=20 μm.

Figure 4F shows a horizontal-type neuron that displays a horizontally oriented fusiform soma and horizontal processes. Horizontal-type neurons were rarely encountered in the present study. Figure 5 shows a histogram of the percent frequency of the cell types of nNOS-IR neurons in the bat visual cortex. Quantitatively, 42.25±2.09% of the nNOS-IR neurons were round- or oval-type neurons, 32.86±2.22% were stellate-type neurons, 19.02±2.02% were vertical fusiform-type neurons, and 5.63±0.84% were horizontal-type neurons. Figure 6 shows the average diameter of each type of nNOS-IR neurons in the bat visual cortex. No obvious differences were found between each type. Quantitatively, the average diameter of the nNOS-IR round- or oval-, stellate-, vertical fusiform-, and horizontal-type neurons in the bat visual cortex were 11.80±1.60 μm, 12.53±2.10 μm, 12.11±1.62 μm, and 11.74±0.86 μm, respectively. The average diameter of the nNOS-IR neurons was 12.1±1.77 μm.

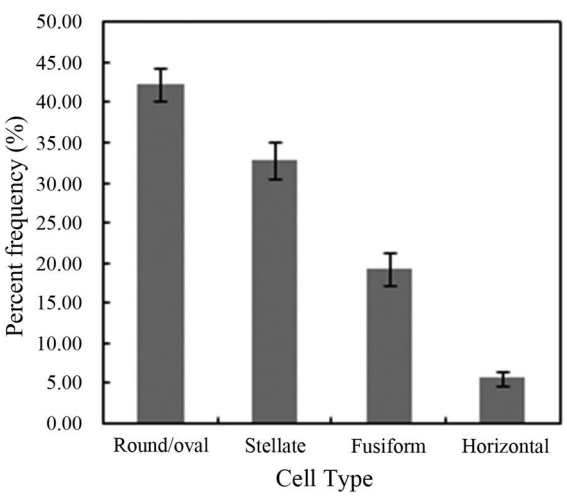

Fig. 5. Histogram of the percent frequency of the cell types of nNOS-IR neurons in the bat visual cortex. Majority of the nNOS-IR neurons were round- or oval-type neurons, and the other major type found were stellate-type neurons. Fusiform- and horizontal-type neurons were rarely encountered in the present study.

The co-localization of nNOS and CB, CR, and PV in the bat visual cortex

To determine whether the nNOS-IR neurons in the bat visual cortex co-localized with CB, CR, or PV, we labeled

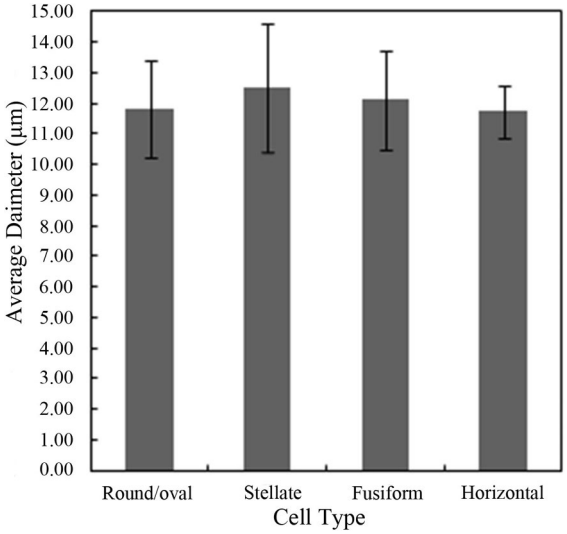

Fig. 6. Histogram of the average diameter of the cell types that were nNOS-IR neurons in the bat visual cortex. No obvious differences were found between each type.

nNOS-IR neurons with FITC and CB-, CR-, or PV-IR neurons with Cy3. We counted the number of nNOS-IR and double-labeled neurons across all layers in three different animals. None of the nNOS-IR neurons were double-labeled with CB, CR, or PV in the bat visual cortex (Fig. 7).

IV. Discussion

The primary purpose of the present study was to confirm if nNOS-IR neurons were localized in a specific layer of the bat visual cortex as in other animals studied. The results showed that two types of nNOS-IR neurons (intensely labeled and weakly labeled) were found throughout the layers of the bat visual cortex, including layer I, and were localized mainly in layer IV and layer VI, respectively. In previous studies in the hamster and monkey visual cortex, the highest density of nNOS-IR neurons was localized to layer VI [1, 26]. In the mouse and rabbit visual cortex, the intensely labeled neurons were more in layer VI, and the weakly labeled, in layer II/III [27]. In rat and human visual cortex, nNOS-IR neurons were localized mainly in layer II/III [16, 29]. In contrast, the distribution of nNOS-IR neurons in the bat visual cortex differed from these patterns. In addition, previous studies showed that nNOS-IR neurons (intensely labeled) in layer I accounted for 1.5% and 2.1% of the neurons in mouse and rabbit, respectively [27], only 0.7% in hamster [26], and were absent in rat [16]. However, in the present study, nNOS-IR neurons (intensely labeled) accounted for 11.76% of the neurons in layer I of the bat visual cortex. Thus, the distribution of nNOS-IR neurons in the visual cortex differs in different species [1, 16, 26, 27, 29], even in the same order. A clear understanding of the functional significance of these different distribution patterns in different species is lacking. However, the results of the present study provide useful evidence on species diversity.

Although the distribution pattern of nNOS-IR neurons in the bat visual cortex differed from other species studied, the morphology was similar to that described in previous studies in humans [29], monkey [1], rat [16], hamster [26], mouse, and rabbit [27] The round- or oval-type neurons made up the largest percentage of nNOS-IR neurons in the visual cortex, and no pyramidal-type neurons were found. Previously, 12 different types of NADPH-d-containing interneurons have been classified based on morphology in human putamen [23]. In this study, four types of nNOS-IR neurons were found in the bat visual cortex: round- or oval-, stellate-, fusiform-, and horizontal-type neurons. These four types are included among the 12. Thus, these findings suggested that nNOS-IR neurons in the bat visual cortex are interneurons.

Because both the synthesis and release of nNOS are calcium-dependent [11, 15, 17, 25], and CBPs also play an important role for calcium buffering, the present study aimed to determine if nNOS-IR neurons also contain CB, CR, or PV in the bat visual cortex. Previous studies have shown that the double-labeling ratio of nNOS with CB, CR, or PV in visual cortex differs among species [1, 16, 26, 27, 29]. For example, among rodents, nNOS-IR neurons and CBPs have been co-localized in the hamster, rat, and mouse visual cortex. In hamster visual cortex, 14.7% and 27.5% of nNOS-IR neurons co-localized with CB and CR, respectively [26]. However, only 1.2% co-localized with CB in rat visual cortex, and none co-localized with CR or PV in rat visual cortex [16]. In mouse, 16.7%, 51.7%, and 25.0% of nNOS-IR neurons contained CB, CR, or PV, respectively [27]. In rabbit, a non-rodent mammal, 92.4% of nNOS-IR neurons contain both nNOS and CB, while only 2.5% co-localized with CR, and none of the nNOS-IR neurons co-localized with PV [27]. In addition, CB, CR, and PV have been widely used as markers of subpopulations of neurons in many brain areas [3, 10]. CB and CR have been identified in the dog [43], mouse [33], hamster [26], and rabbit [32] visual cortex. In these animals, majority of the CB-IR neurons were multipolar stellate- and round- or oval-type neurons, while most of CR-IR neurons were vertical fusiform-type neurons. PV-IR neurons have been localized in the dog [43] and rabbit [32] visual cortex. The two principal neuronal types in these animals were multipolar stellate-type neurons and round- or oval-type neurons. These results showed that CB-, CR-, and PV-IR neurons were localized in specific cell types. The function of CBPs in the visual cortex is not clear. They are suggested to be closely related to many neurological disorders [2, 4, 9, 13, 18, 19, 20, 28, 34]. However, in the present study, nNOS-IR neurons did not co-localize with CB, CR, or PV in the bat visual cortex. These findings suggest that nNOS-IR neurons are a specific subpopulation of interneurons in the bat visual cortex.

In summary, the results indicate that nNOS-IR neurons

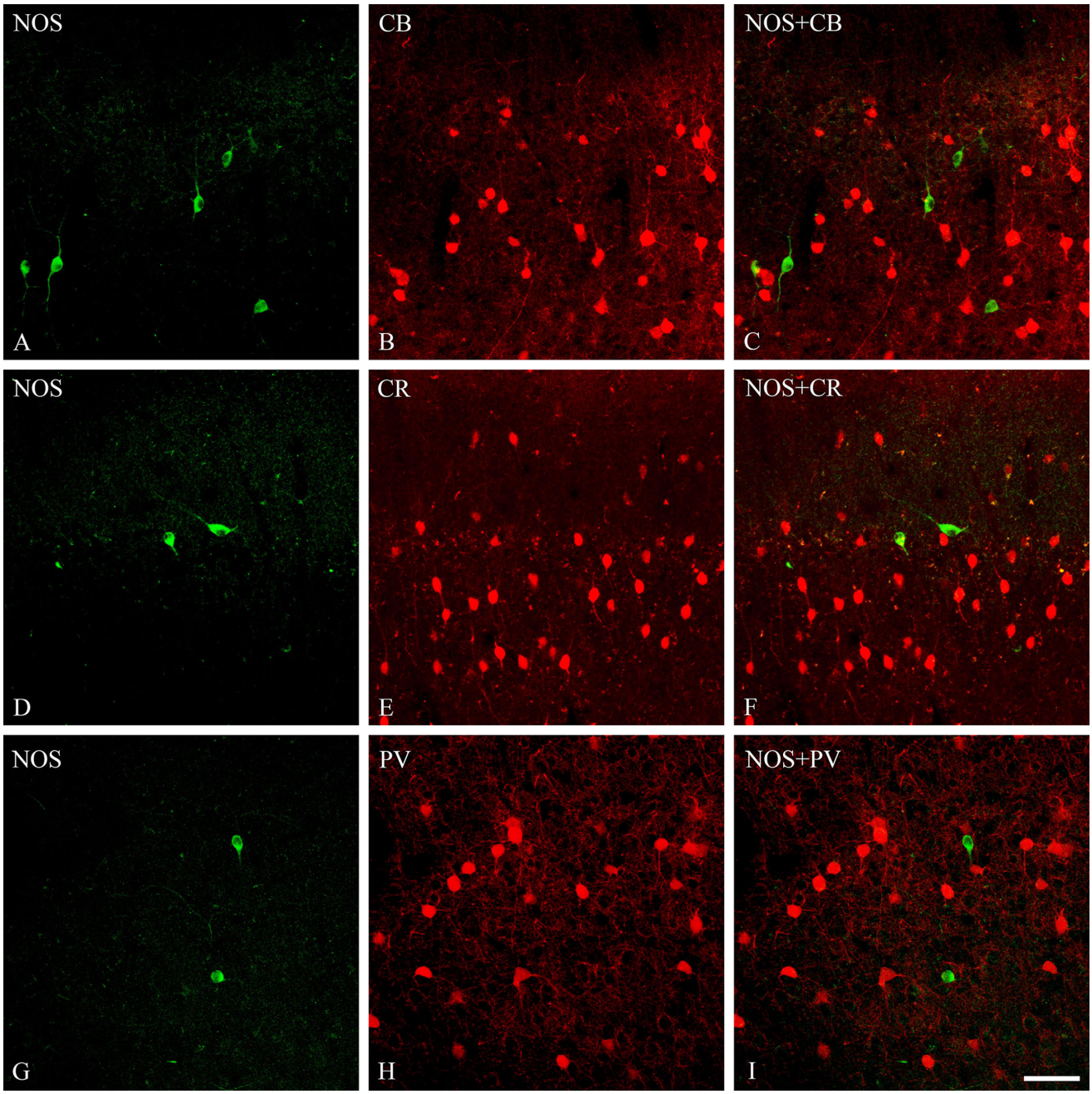

Fig. 7. Fluorescence confocal photomicrographs of the bat visual cortex immunolabeled for (**A, D, G**) nNOS and (**B, E, H**) CBPs. (**C**) Superimposition of images of nNOS- and CB-IR neurons. (**F**) Superimposition of images of nNOS- and CR-IR neurons. (**I**) Superimposition of images of nNOS- and PV-IR neurons. None of the nNOS-IR neurons was double-labeled with CB, CR, or PV. Bar=50 μm.

in the bat visual cortex were localized mainly in layer IV (intensely labeled) and layer VI (weakly labeled). The cell types show a different distribution patterns but similar morphology as reported in other species. The laminar differences between bat and other species may provide a useful clue for further understanding species diversity and the functional diversity of NO in the visual cortex. The morphology of nNOS-IR neurons suggests that most of these in the bat visual cortex are interneurons. However, contrary to previous findings, the nNOS-IR neurons did not show any co-localization with CB, CR, or PV in this study. Because NO is an important non-synaptic neurotransmitter synthesized by nNOS in neurons of the central nervous system, the presence of nNOS in the bat visual cortex could provide strong evidence for the visual ability of bats.

V. Acknowledgments

We thank Cactus Communications for proofreading the manuscript. This work was supported by Basic Science

Research Program through the National Research Foundation of Korea (NRF) funded by Ministry of Education (NRF-2011-0024882).

VI. References

1. Aoki, C. S., Fenstemaker, S., Lubin, M. and Go, C. G. (1993) Nitric oxide synthase in the visual cortex of monocular monkeys as revealed by light and electron microscopic immunocytochemistry. *Brain Res.* 620; 97–113.
2. Baglietto-Vargas, D., Moreno-Gonzale, I., Sanchez-Varo, R., Jimenez, S., Trujillo-Estrada, L., Sanchez-Mejias, E., Torres, M., Romero-Acebal, M., Ruano, D., Vizuete, M., Vitorica, J. and Gutierrez, A. (2010) Calretinin interneurons are early targets of extracellular amyloid-beta pathology in *PS1/AbetaPP Alzheimer* mice hippocampus. *J. Alzheimers Dis.* 21; 119–132.
3. Baimbridge, K. G., Celio, M. R. and Rogers, J. H. (1992) Calcium-binding proteins in the nervous system. *Trends Neurosci.* 15; 303–308.
4. Barraclough, R. (1998) Calcium-binding protein S100A4 in health and disease. *Biochim. Biophys. Acta* 1448; 190–199.
5. Bear, M. F., Connors, B. W. and Paradiso, M. A. (2007) Neurotransmitter systems. In "Neuroscience: Exploring the Brain 3rd ed.", ed. by M. F. Bear, B. W. Connors and M. A. Paradiso, Lippincott Williams & Wilkins, Baltimore, pp. 133–166.
6. Bonhoeffer, T., Staiger, V. and Aertsen, A. (1989) Synaptic plasticity in rat hippocampal slice cultures: local "Hebbian" conjunction of pre- and postsynaptic stimulation leads to distributed synaptic enhancement. *Proc. Natl. Acad. Sci. U S A* 86; 8113–8117.
7. Bredt, D. S. and Snyder, S. H. (1989) Nitric oxide mediates glutamate-linked enhancement of cGMP levels in the cerebellum. *Proc. Natl. Acad. Sci. U S A* 86; 9030–9033.
8. Bredt, D. S. and Snyder, S. H. (1990) Isolation of nitric oxide synthetase, a calmodulin-requiring enzyme. *Proc. Natl. Acad. Sci. U S A* 87; 682–685.
9. Byun, K., Kim, D., Bayarsaikhan, E., Oh, J., Kim, J., Kwak, G., Jeong, G. B., Jo, S. M. and Lee, B. (2013) Changes of calcium binding proteins, c-Fos and COX in hippocampal formation and cerebellum of Niemann-Pick, type C mouse. *J. Chem. Neuroanat.* 52; 1–8.
10. Celio, M. R. (1990) Calbindin D-28k and parvalbumin in the rat nervous system. *Neuroscience* 35; 375–475.
11. Dawson, T. M. and Snyder, S. H. (1994) Gases as biological messengers: nitric oxide and carbon monoxide in the brain. *J. Neurosci.* 14; 5147–5159.
12. Dawson, V. L. and Dawson, T. M. (1996) Nitric oxide actions in neurochemistry. *Neurochem. Int.* 29; 97–110.
13. Ferrer-Acosta, Y., Rodríquez-Cruz, E. N., Orgnge, F., De Jesús-Cortés, H., Madera, B., Vaquer-Alicea, J., Ballester, J., Guinel, M. J., Bloom, G. S. and Vega, I. E. (2013) EFhd2 is a novel amyloid protein associated with pathological tau in Alzheimer's disease. *J. Neurochem.* 125; 921–931.
14. Finkel, L. H. and Edelman, G. M. (1987) Population rules for synapses in networks. In "Synaptic Function", ed. by G. M. Edelman, W. E. Gall and W. M. Cowan, Wiley, New York, pp. 711–757.
15. Gally, J. A., Montaque, P. R., Reeke, G. N. Jr. and Edelman, G. M. (1990) The No hypothesis: possible effects of a short-lived, rapidly diffusible signal in the development and function of the nervous system. *Proc. Natl. Acad. Sci. U S A* 87; 3547–3551.
16. Gonchar, Y. and Burkhalter, A. (1997) Three distinct families of GABAergic neurons in rat visual cortex. *Cereb. Cortex* 7; 347–358.
17. Griffith, O. W. and Stuehr, D. J. (1995) Nitric oxide synthases: Properties and catalytic mechanism. *Annu. Rev. Physiol.* 57; 707–736.
18. Hayashi, S., Amari, M. and Okamoto, K. (2013) Loss of calretinin- and parvalbumin- immunoreactive axon in anterolateral columns beyond the corticospinal tracts of amyotrophic lateral sclerosis spinal cords. *J. Neurol. Sci.* 331; 61–66.
19. Heizmann, C. W. and Braun, K. (1995) Calcium Regulation by Calcium-binding Proteins in Neurodegenerative Disorders. Springer-Verlag, Heidlberg.
20. Hurley, M. J., Brandon, B., Gentleman, S. M. and Dexter, D. T. (2013) Parkinson's disease is associated with altered expression of CaV1 channels and calcium-binding proteins. *Brain* 136; 2077–2097.
21. Jeon, Y. K., Kim, T. J., Lee, J. Y., Choi, J. S. and Jeon, C. J. (2007) AII amacrine cells in the inner nuclear layer of bat retina: identification by parvalbumin immunoreactivity. *Neuroreport* 18; 1095–1099.
22. Jeong, S. J., Kim, H. H., Lee, W. S. and Jeon, C. J. (2014) Immunocytochemical localization of calbindin D28k, calretinin and parvalbumin in bat superior colliculus. *Acta Histochem. Cytochem.* 47; 113–123.
23. Johannes, S., Reif, A., Senitz, D., Riederer, P. and Lauer, M. (2003) NADPH-diaphorase staining reveals new types of interneurons in human putamen. *Brain Res.* 980; 92–99.
24. Kim, T. J., Jeon, Y. K., Lee, J. Y., Lee, E. S. and Jeon, C. J. (2008) The photoreceptor populations in the retina of the greater horseshoe bat Rhinolophus ferrumequinum. *Mol. Cells* 26; 373–379.
25. Kiss, J. P. and Vizi, E. S. (2001) Nitric oxide: a novel link between synaptic and nonsynaptic transmission. *Trends Neurosci.* 24; 211–215.
26. Lee, J. E., Ahn, C. H., Lee, J. Y., Chung, E. S. and Jeon, C. J. (2004) Nitric oxide synthase and calcium-binding protein-containing neurons in the hamster visual cortex. *Mol. Cells* 18; 30–39.
27. Lee, J. E. and Jeon, C. J. (2005) Immunocytochemical localization of nitric oxide synthase-containing neurons in mouse and rabbit visual cortex and co-localization with calcium-binding proteins. *Mol. Cells* 19; 408–417.
28. Leuba, G., Kraftsik, R. and Saini, K. (1998) Quantitative distribution of parvalbumin, calretinin, and calbindin D-28k immunoreactive neurons in the visual cortex of normal and Alzheimer cases. *Exp. Neurol.* 152; 278–291.
29. Lüth, H. J., Hedlich, A., Hilbig, H., Winkelmann, E. and Mayer, B. (1994) Morphological analyses of NADPH diaphorase/nitric oxide synthase positive structures in human visual cortex. *J. Neurocytol.* 23; 770–782.
30. Mattson, M. P., Lee, R. E., Adams, M. E., Guthrie, P. B. and Kater, S. B. (1988) Interactions between entorhinal axons and target hippocampal neurons: a role for glutamate in the development of hippocampal circuitry. *Neuron* 1; 865–876.
31. Müller, B., Glösmann, M., Peichl, L., Knop, G. C., Hagemann, C. and Ammermüller, J. (2009) Bat eyes have ultraviolet-sensitive cone photoreceptors. *PLoS One* 4; e6390.
32. Park, H. J., Lee, S. N., Lim, H. R., Kong, J. H. and Jeon, C. J. (2000) Calcium-binding proteins calbindin D28K, calretinin, and parvalbumin immunoreactivity in the rabbit visual cortex. *Mol. Cells* 10; 206–212.
33. Park, H. J., Kong, J. H., Kang, Y. S., Park, W. M., Jeong, S. A., Park, S. M., Lim, J. K. and Jeon, C. J. (2002) The distribution and morphology of calbindin D28k- and calretinin-immunoreactive neurons in the visual cortex of mouse. *Mol. Cells* 14; 143–149.
34. Reynolds, G. P., Zhang, Z. J. and Beasley, C. L. (2001) Neurochemical correlates of cortical GABAergic deficits in schizophrenia: selective losses of calcium binding protein

immunoreactivity. *Brain Res Bull.* 55; 579–584.
35. Rogers, J. H. (1987) Celretinin: a gene for a novel calcium-binding protein expressed principally in neurons. *J. Cell Biol.* 105; 1343–1353.
36. Schäfer, B. W. and Heizmann, C. W. (1996) The S100 family of EF-hand calcium-binding proteins functions and pathology. *Trends Biochem. Sci.* 21; 134–140.
37. Schmidt, H. H., Gagne, G. D., Nakane, M., Pollock, J. S., Miller, M. F. and Murad, F. (1992) Mapping of neural nitric oxide synthase in the rat suggests frequent co-localization with NADPH diaphorase but not with soluble guanylyl cyclase, and novel paraneural functions for nitrinergic signal transduction. *J. Histochem. Cytochem.* 40; 1439–1456.
38. Schulman, H. (1997) Nitric oxide: a spatial second messenger. *Mol. Psychiatry* 2; 296–299.
39. Vizi, E. S. and Kiss, J. P. (1998) Neurochemistry and pharmacology of the major hippocampal transmitter systems: synaptic and nonsynaptic interactions. *Hippocampus* 8; 566–601.
40. Vizi, E. S. (2000) Role of high-affinity receptors and membrane transporters in nonsynaptic communication and drug action in the central nervous system. *Pharmacol. Rev.* 52; 63–89.
41. Winsky, L., Nakata, H., Martin, B. M. and Jacobowitz, D. W. (1989) Isolation, partial amino acid sequence, and immuno-histochemical localization of a brain-sepecific calcium-binding prtein. *Proc. Natl. Acad. Sci. U S A* 86; 10139–10143.
42. Winter, Y., López, J. and Von, H. O. (2003) Ultraviolet vision in a bat. *Nature* 425; 612–614.
43. Yu, S. H., Lee, J. Y. and Jeon, C. J. (2011) Immunocytochemical localization of calcium-binding proteins, calbinding D28k-, calretinin-, and parvalbumin- containing neurons in the dog visual cortex. *Zoolog. Sci.* 28; 694–702.
44. Zhao, H. B., Xu, D., Zhou, Y. Y., Flanders, J. and Zhang, S. Y. (2009) Eudution of opsin genes reveals a functional role of vision in the echolocating little brown bat (Myotis lucifugus). *Biochem. Syst. Ecol.* 37; 154–161.